Appl. Phys. A 66, S993–S997 (1998)

Applied Physics A
Materials
Science & Processing

A UHV STM for in situ characterization of MBE/CVD growth on 4-inch wafers

O. Leifeld[1,2], **B. Müller**[1,*], **D.A. Grützmacher**[2], **K. Kern**[1]

[1] Institut de Physique Expérimentale, EPF Lausanne, CH-1015 Lausanne, Switzerland
[2] Labor für Mikro- und Nanostrukturen, Paul Scherrer Institut, CH-5232 Villigen-PSI, Switzerland

Received: 25 July 1997/Accepted: 1 October 1997

Abstract. A UHV STM has been designed for combination with a multipurpose MBE/UHV-CVD system. A small UHV chamber containing the STM is attached to the load lock of the MBE chamber for sample transfer. For high-resolution measurements, the STM chamber is detached from the MBE/CVD machine to reduce the noise level and to avoid the transmission of vibrations. Vibration isolation is provided by laminar flow isolators carrying the whole chamber as well as by a spring/eddy current assembly damping the sample holder and the STM. Emphasis is put on the suppression of eigenmodes of the 4-inch wafer. The STM itself, based on the 'Beetle'-microscope with an inchworm motor for tip approach, is placed directly on the wafer. The area which can be investigated corresponds to $\sim 40\,\mathrm{cm}^2$. The instrument performance is demonstrated for Si(111) and Si(001) surfaces.

Scanning tunneling microscopy (STM) has become a powerful tool in surface science, characterizing metal [1] and semiconductor [2] surfaces from microscopic to mesoscopic scales. However, most STMs are restricted to rather small sample sizes of $\sim 1\,\mathrm{cm}^2$, limiting their application mainly to custom-made sample preparation and growth systems designed entirely for research applications. In device-orientated silicon technology the minimum standard sample size is that of a 4-inch wafer, serving as base material for all kinds of processing steps. The combination of STM with molecular beam epitaxy (MBE) or chemical vapor deposition (CVD) machines that process such large samples is complicated, since the pumps of the growth chambers are inherent sources of vibration. Moreover, for large thin wafers eigenmodes can be excited, which make high-resolution measurements difficult or even impossible. The implementation of an STM in the growth chamber thus requires that MBE or CVD operation must be stopped during STM-investigations [3].

* Present address: Institute of Quantum Electronics, Nonlinear Optics Laboratory, Swiss Federal Institute of Technology, CH-8093 Zürich, Switzerland

In this paper, we demonstrate that the problems mentioned above can be overcome. We have realized a combination of a powerful STM with our MBE/UHV-CVD machine that consists of a Balzers UMS 500 MBE chamber combined with a UHV-CVD reactor and sample transfer system, all for use with 4-inch samples. The STM is contained in a small transportable ultrahigh vacuum (UHV) chamber attached via a loadlock to the sample transfer chamber of the MBE/CVD system. The prepared wafer is then transferred from the growth chamber to the STM chamber by means of the transfer system of the MBE/CVD machine, thus avoiding additional sample handling by space-consuming transfer rods or wobble sticks. To avoid noise problems due to mechanical vibrations, mainly caused by the growth system, the STM chamber is detached from the growth system and moved to another room for high-resolution measurements. Once moved to the other room, vibration isolation is done by laminar flow isolators (Newport I2000 series) carrying the whole chamber. Inside the vacuum vessel a spring/eddy current assembly that suspends both the sample and the STM provides additional effective vibration damping. Wafer eigenmodes are suppressed by a special design of the sample stage. The STM itself is based on the Beetle, originally proposed by Besocke [4]. Tip approach is realized by an Inchworm motor.

A particularly important feature of our design is the ability to probe a large area of the wafer, allowing us to examine the surface within a diameter of more than 60 mm. This is especially important for the characterization of the homogeneity across the wafer.

1 Vacuum system

The vacuum system consists of two parts (the main chamber with the STM and the loadlock for the connection to the MBE/CVD system) separated by a UHV gate valve. The main chamber is a standard CF150 cross. The STM with damped sample holder is mounted on a CF 150 flange fixed at the top flange of the chamber. Two side flanges contain viewports in order to inspect the STM. The lower flange carries an ion pump (MECA2000 PIDG200) with a titanium

sublimation pump incorporated. The rough pumping is done via the loadlock, which is equipped with a turbomolecular drag pump (Balzers TMU065). The volume of the loadlock is kept as small as possible to achieve fast pump-down times, although CF150 flanges are obligatory for 4-inch sample transfer. The base pressure corresponds to 1×10^{-10} mbar in the STM chamber and 1×10^{-9} mbar in the loadlock after bakeout.

The vacuum system is mounted on a compact trolley (length 90 cm, width 65 cm) which also contains power supplies for the pumps and pressure measurement. Thus the whole system can be moved from one lab to another, connected to the power line by a single cable. The height of the chamber center axis with respect to the floor can be adjusted between 95 cm and 145 cm. This is necessary to adapt to the transfer flange height of the MBE/CVD system and to be able to pass through doors. The chamber can be lowered onto a custom-made stone plate that floats on the laminar flow isolators. The isolators suppress the coupling of building vibrations.

2 STM setup

The cross-sectional drawing, together with the 3D view, in Fig. 1 shows the simple construction of the STM head. Three identical piezo tubes (2) with four quadrant electrodes on the outer circumference are glued to the STM body (1) with conductive UHV epoxy, each of them carrying a ruby ball (3) at its end. With these ruby balls the STM is lowered directly onto the wafer surface (8) at the desired position. This coarse positioning is done by a standard UHV *xyz*-manipulator, with a range of ± 25 mm in the *xy*-plane and 100 mm in the *z*-direction. In addition, the STM can travel around on the surface for several millimeters in each direction by means of inertial motion if a sawtooth-like voltage is applied to the electrodes of the three outer piezos (slip-stick motion). A d.c. offset voltage of ± 200 V at these piezos allows exact positioning of the tip within $\sim 2.5\,\mu$m. We consider the sample surface damage by the three ruby balls to be insignificant in terms of the negligible probability of involuntarily investigating an area where one of the legs had already been.

In the center of the microscope a UHV inchworm motor (4) (Burleigh UHVL Inchworm Motor) is mounted for tip approach. It is fabricated entirely from ceramics. The inchworm shaft has a travel length of 10 mm with a step resolution of 1 nm. Inside this hollow shaft the fourth piezo tube (5) responsible for the scanning motion and tip-sample distance control is inserted. This is glued to a ceramic tube (6), which is centered inside the inchworm shaft by means of two centering rings, thus avoiding the bending modes of the rather long inner tube. Inside it is covered with a metal mesh serving as shielding for the tunneling current. The upper end of this ceramic tube is glued to a flange-like aluminum plate that is screwed against an aluminum ring attached to the upper end of the inchworm shaft. This assembly offers two advantages: first, in contrast to a scan piezo glued directly to an inchworm shaft, one can relatively easily separate the scan piezo from the inchworm for service in case of any problems, without the risk of destroying the inchworm. Second, as both the inchworm and the tube, which

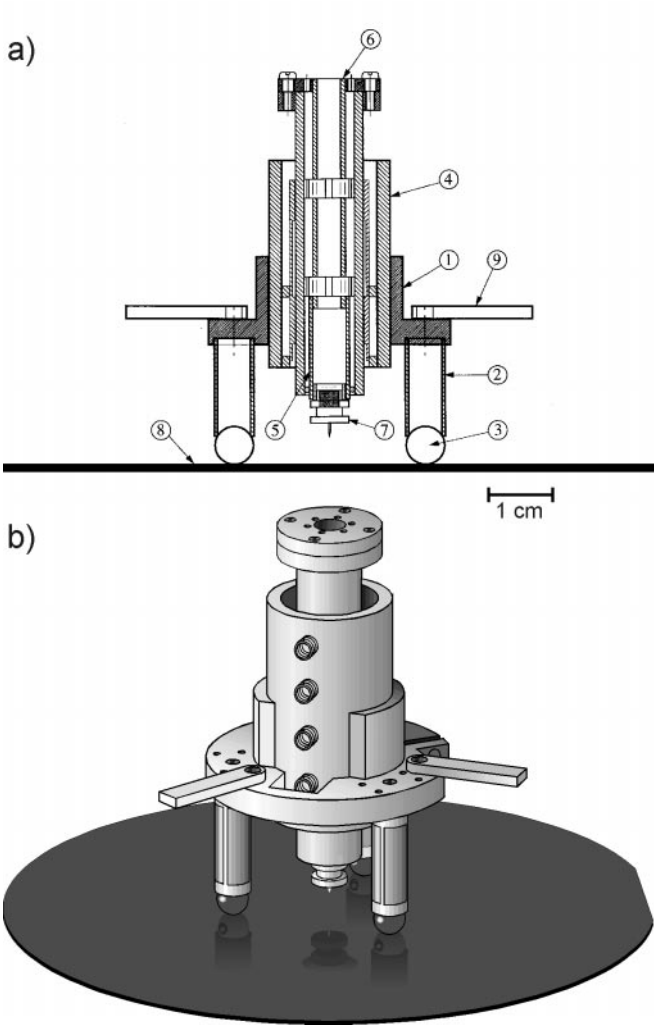

Fig. 1. a Scheme of the STM head: (1) STM body, (2) piezo tube, (3) ruby ball, (4) inchworm, (5) scan piezo, (6) ceramic tube with centering rings and Al flange plate, (7) magnetically fixed tip holder, (8) Si wafer, (9) levers for lifting the microscope. **b** Three-dimensional view of the STM on the Si sample

holds the scan piezo, are made from ceramics, the compensation for thermal drift in the tip-sample distance, which is achieved with a normal beetle design, is still valid to a first-order approximation.

All electrical connections to the STM are made of 50 μm capton-isolated copper wires. We use a 250 μm diameter polycrystalline tungsten wire for the tunneling tips. These are electrochemically etched in NaOH solution. The tip holder (7) comprises a small CoSm magnet that holds it in place at the end of the scan piezo. Thus the tip holder is exchangeable without breaking the ultrahigh vacuum. New tips are introduced via the loadlock with a transfer rod holding a tip magazine for three tips. The exchange is accomplished by moving the microscope with the *xyz*-manipulator so that the tip holder is pushed into a fork of the tip magazine. Then the microscope is retracted and the tip holder is removed from the scan piezo.

The STM-sample stage can receive a wafer directly from the sample handler of the MBE/CVD system. It includes the spring suspension and eddy current damping. A photograph is shown in Fig. 2.

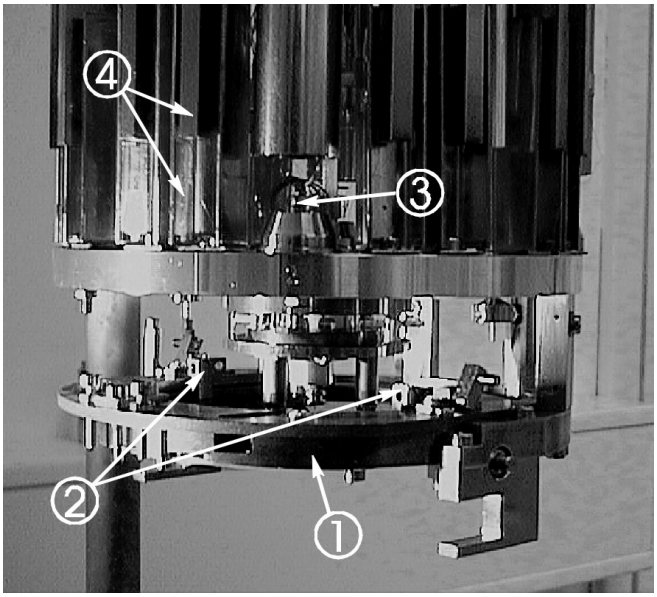

Fig. 2. Sample stage in measuring position. The STM is positioned on the wafer. The drawer-like Ta sample holder (1) can be turned by 180° for sample introduction. The wafer is clamped at two points by the Ta levers (2). The whole stage is suspended with springs (3) and damped by eddy currents. The copper pieces and magnets (4) are visible on top of the sample stage

In the MBE system the wafer is moved and processed upside down, which means that the surface of interest is on the bottom side. The wafer resides in a support ring also made of silicon, in order to avoid contact with stainless steel parts. This support ring, 115 mm in diameter, can be transferred to the STM by the sample handler, consisting of a simple fork with a depression holding the ring. The fork only moves horizontally and can take two defined vertical positions. In the upper position the support ring is pushed into the drawer-like STM sample holder (1). The wafer is still upside down. After the sample handler fork is withdrawn, the STM sample holder is turned by 180° by means of a rotary UHV feedthrough, which allows access to the surface for the STM from above (Fig. 2). During this turn, two spring-loaded levers (2) push against the wafer and clamp it at two points near the edge to the bottom plate of the sample holder. This plate is machined to be accurately plane, so that the wafer backside entirely touches it. In this way wafer vibrations are effectively suppressed, as will be shown later. Like all parts of the sample stage coming into contact with the silicon sample support ring or the wafer, the bottom plate and the clamping levers are manufactured from pure tantalum in order to prevent wafer contamination.

During the transfer the sample stage is rigidly fixed in the transfer position. For STM measurement, before the STM is lowered onto the sample surface, the support is removed and the sample stage is suspended by four soft spiral springs (3). These springs have a nominal extension of 250 mm under load, thus leading to an eigenfrequency of 1 Hz for the stage. On top of the stage, 16 U-shaped copper pieces are fixed at the circumference for eddy current damping. Each of them embraces a fixed 1 T CoSm magnet (4). This assembly leads to a Q factor of 12 in the vertical direction and a Q of 4 for horizontal and torsional movements of the stage. Thus the suspension provides effective isolation against mechanical and acoustical noise from the outside.

3 Wafer eigenmodes

An important source of vibration in scanning tunneling microscopy is the STM itself. The scan motion, a slow ramp usually generated stepwise by a digital-analog converter, and the z-piezo movement due to distance regulation by the feedback circuit contain a wide spectrum of frequencies. In consequence, the amplification of any of these frequencies within the sample holder and STM must be avoided. The most effective way is to build the STM and sample unit as compactly and rigidly as possible, with high eigenfrequencies of all components. However, in our case the compactness is rather limited by the large sample size. While the size and rigidity of the STM head is no problem, and even the sample holder could be made sufficiently rigid by choice of material thickness, it is the silicon wafer that remains problematic. Due to its rather small thickness (typically between 0.3 mm and 0.8 mm) and its large diameter, it shows low-frequency eigenmodes. Theory predicts the eigenfrequencies of a circular plate of thickness s and radius r as [5]:

$$\nu_{\mathrm{mn}} = \frac{\pi s}{2r^2}\beta_{\mathrm{mn}}^2\sqrt{\frac{E}{3\rho(1-\mu^2)}} \tag{1}$$

with elastic modulus E, density ρ and Poisson number μ. The β_{mn} denote the coefficients for the non-harmonic eigenmodes with m nodes in the radial direction and n in the azimuthal direction. The boundary conditions are given by fixing around the edge of the circumference. The first mode, ν_{01}, with $\beta_{01} = 1.015$, has one maximum in the center of the plate and the second, ν_{11}, with $\beta_{11} = 1.468$, has two maxima and one node across the middle of the wafer. For a 4-inch silicon wafer with a thickness of 0.5 mm, (1) yields frequencies of 630 Hz and 1315 Hz respectively.

In order to verify the appearance of the eigenmodes, we positioned the STM at the center of a wafer that was supported only around its edge. One of the three outer piezos was excited by an a.c. voltage of 8 V_{pp} to vibrate along its symmetry axes (perpendicular to the wafer surface). The response signal of the system wafer/STM was taken at a second outer piezo and detected with a lock-in amplifier. The frequency spectrum obtained is shown in the upper curve in Fig. 3. Its main feature is the resonance peak at 1280 Hz. We attribute this peak to the second eigenmode ν_{11} of the wafer, as the excited piezo is located slightly away from the wafer center. So the excitation of this mode is probable. A second peak is visible at 1860 Hz and a third one, although smaller, at 105 Hz. Their origin could not be determined definitely. We believe, that they occur due to the presence of the STM on the vibrating wafer, as both STM and wafer cannot be considered to be independent.

These resonances give rise to periodic perturbations in the images. Therefore we were looking for a simple way to suppress these modes. This is done by supporting the wafer by simply putting it on a thick, rigid tantalum plate and clamping it as mentioned above. The vibration spectrum taken in this configuration is plotted in the lower curve in Fig. 3. The peak at 1280 Hz has completely disappeared, which demonstrates

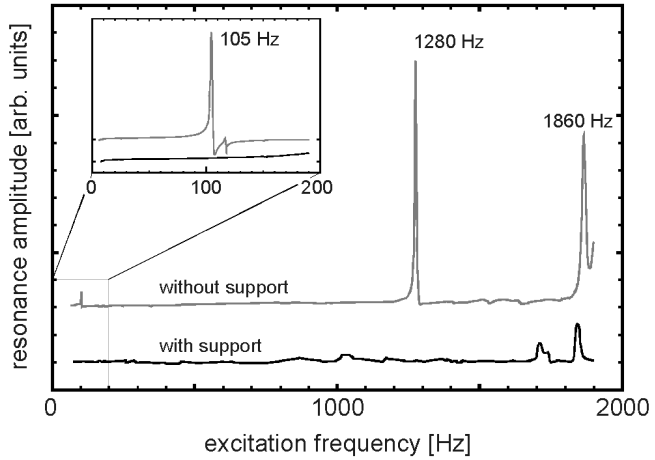

Fig. 3. Resonance spectra of the ensemble STM/wafer demonstrating the wafer eigenmodes. For a wafer supported only at its circumference (*upper curve*) distinct resonance peaks appear, whereas for a wafer clamped on the flat surface of the sample stage (*lower curve*) they disappear

the efficient suppression of the eigenmode. Even the peak at 105 Hz has vanished, and the one at 1860 Hz has decreased in amplitude by a factor of three, indicating that these were at least partly due to the free wafer vibrations.

4 STM performance

In order to demonstrate the capabilities of our 4-inch wafer STM we first investigated the Si(111) and Si(001) surfaces. Si(111) samples were cleaned by an RCA clean [6] followed by an HF dip for H passivation before being transferred to the MBE growth chamber. There they were heated to 600 °C for 30 min in order to desorb the hydrogen, and subsequently to 950 °C for 10 min for desorption of other possible contaminants. This treatment results in a clear 7×7 reconstruction observed by RHEED. A similar procedure was used for the Si(001) samples (3 min at 600 °C followed by 30 min at 900 °C), leading to the 2×1 RHEED pattern of clean Si(001). After cooling down to room temperature, samples were transferred to the STM.

On Si(111) the 7×7 reconstruction with its adatoms and the cornerholes could routinely be resolved. We used the unit cell of this reconstruction to calibrate the scan ranges of our STM. The *z*-motion of the scan piezo was calibrated at the steps between bilayers, which exhibit a height of 3.13 Å on Si(111). A maximum corrugation of 50 nm can be measured without damaging the tip.

Figure 4a shows a 150-nm Si film grown on Si(111) 7×7 at 600 °C with a growth rate of 1 Å/s. One can see the formation of domains containing different reconstructions of dimer-adatom-stacking fault (DAS) structures [7] (5×5, 7×7, 9×9). This mixture is typical for low-temperature homoepitaxy on Si(111) 7×7 [8]. The individual adatoms are imaged even at the boundaries of the bilayer steps, indicating the perfect lateral resolution of our instrument. The resolution in the *z*-direction is better than 0.1 Å, estimated by comparing the different apparent heights of the faulted and unfaulted halves (i.e. those with and without underlying stacking faults, respectively) with the known bilayer step height. This can be seen in the inset of Fig. 4a, where the faulted halves (f) of

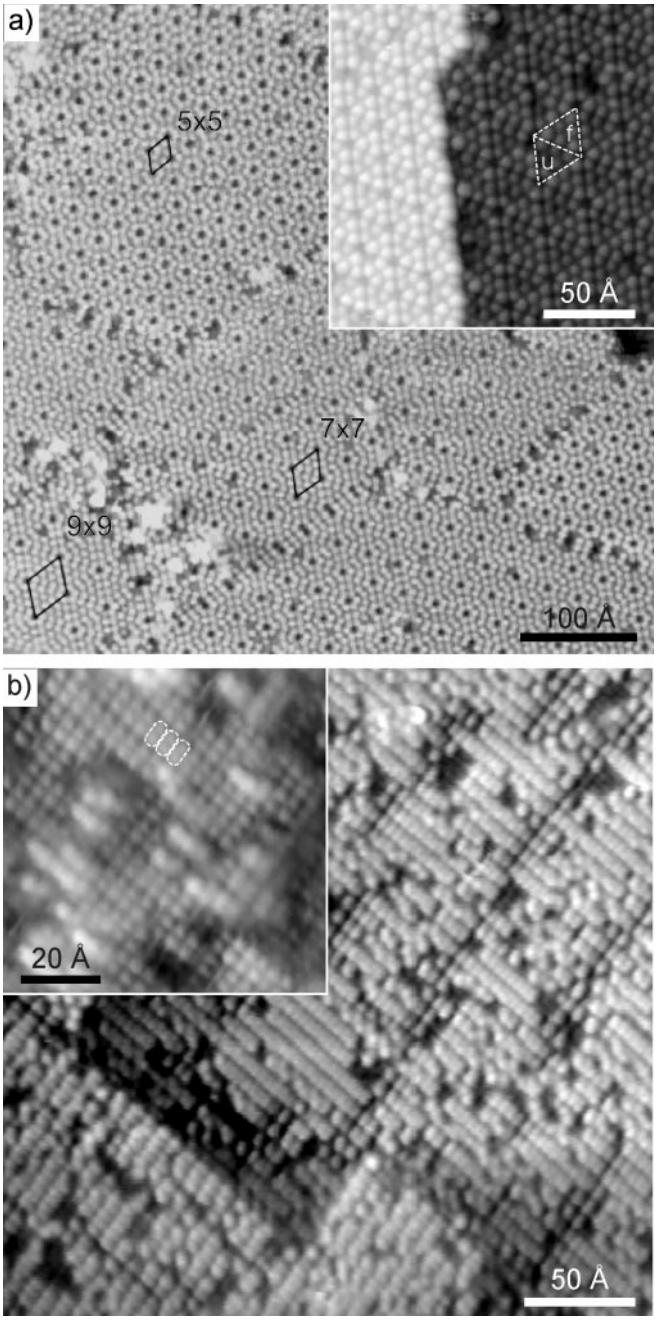

Fig. 4. a STM images of the surface of a 150 nm thick layer grown at 600 °C on a Si(111) 7×7 reconstructed surface taken at -1.9 V tip bias and 0.1 nA ($+0.85$ V and 0.5 nA for the inset). The single adatoms and domains of 5×5, 7×7 and 9×9 reconstructions can be clearly distinguished. **b** Si(001) substrate after heat treatment in UHV. The dimers within the rows are well resolved at a tip bias of $+1.88$ V and 0.2 nA. The inset image shows the unoccupied states with additional depressions within the dimers at a tip bias of -0.85 V and 0.2 nA at higher magnification

the 7×7 and 5×5 unit cells appear a little brighter than the unfaulted ones (u).

Figure 4b represents a Si(001) surface directly after substrate preparation. Single dimers are clearly resolved within the dimer rows (corrugation ~ 0.1 Å) when tunneling from occupied sample states. The inset of Fig. 4b is taken at a positive sample bias, hence tunneling to unoccupied states. In this empty state image, where additional depressions appear

in the center of the dimer rows, the symmetry of the unoccupied antibonding states of the dimers is visible [9], as it is frequently observed with very sharp tips. This image also demonstrates the high resolution, although the surface exhibits a rather large number of defects, seen as missing dimers or as starting points for dimer buckling. This is probably due to insufficient sample cleaning, resulting in carbon contamination.

5 Conclusion

We designed a UHV STM for in situ studies of 4-inch wafers that is compatible with a commercial MBE/UHV-CVD system. In contrast with other large sample STMs, where the sample is put on top of the STM, we can probe areas one or two orders of magnitude larger. (For the large sample STM (LSSTM) of Omicron Vakuumphysik GmbH an accessible area of 1 cm^2 is given. The 3-inch wafer STM of Butz et al. [3], where the wafer is put on top of the three STM piezos, can access no more than 0.6 cm^2, as they are only 12 mm apart.) We have demonstrated atomic resolution on Si(111) and Si(001) after a drastic reduction of the wafer eigenmodes. This reduction can only be done by rigid support of the wafer with a plate, resulting in a heavy sample unit. This fact, and the demand for the large accessible area, necessitates placing the STM on top.

The combination of a powerful STM with an MBE/UHV CVD system enables us to study the different aspects of MBE/CVD growth, including substrate treatment, on an atomic scale.

References

1. F. Besenbacher: Rep. Prog. Phys. **59**(12), 1737 (1996)
2. H. Neddermeyer: Rep. Prog. Phys. **59**(6), 701 (1996)
3. R. Butz, H. Wagner, K. Besocke: Thin Solid Films **183**, 339 (1989)
4. K. Besocke: Surf. Sci. **181**, 145 (1987)
5. P.M. Morse, K.U. Ingard: *Theoretical Acoustics* (Princeton University Press, Princeton 1986) p. 216
6. W. Kern, D. Puotinen: RCA Rev. **31**, 187 (1970)
7. K. Takayanagi, Y. Tanishiro, M. Takahashi, S. Takahashi: J. Vac. Sci. Technol. A **3**, 1502 (1985)
8. U. Köhler, J.E. Demuth, R.J. Hamers: J. Vac. Sci. Technol. A **7**, 2860 (1989)
9. R.J. Hamers, Ph. Avouris, F. Bozso: Phys. Rev. Lett. **59**, 2071 (1887)